

Investigation of Damper Valve Dynamics Using Parametric Numerical Methods

F.G. Guzzomi, P.L. O'Neill and A.C.R. Tavner

School of Mechanical Engineering
University of Western Australia, 6009 AUSTRALIA

Abstract

The objectives of this study are to identify the dynamics of a Tenneco Automotive hydraulic damper valve and to predict valve performance. Accurate simulations of damper valve performance can be used to improve valve designs without the expense of physical testing. The Tenneco damper valve consists of thin shims and a spring preloaded disc that restricts fluid from exiting the main flow orifices. The deflection of the shims and spring are dependent on the flow-rate through the valve. The pressure distribution acting on the deformable valve components is investigated numerically using a dynamic modelling technique. This technique involves sequential geometry and simulation updating, while varying both the geometry and flow-rate. The valve deflection is calculated by post-processing the pressure distribution. Valve performance can be predicted by coupling the valve deflection with CFD pressure results.

Introduction

For race engineers, the ability to predict damper performance is critical to the setup of dampers for road conditions that vary between races. Similarly, automotive engineers studying the noise, vibration and harshness (NVH) of production cars select damper valving to improve ride comfort without compromising handling. Accurate simulations of dampers and their valves can be used to improve damper performance without the expense of physical testing.

Damper valves are a complex, fully coupled, hydraulic system, where flow, valve displacement and pressure differential interact. Traditional mathematical damper models struggle to capture the inhomogeneous fluid pressure acting on the deformable valve structure [23]. The pressure influences the coupling between valve displacement and flow, which governs the overall damping. The pressure is inhomogeneous due to stagnation effects that occur as the fluid enters the region below the valve and as the fluid flows out of the small gap generated by valve deflection. Finally the re-circulation from the valve pressure drop contributes to the inhomogeneity [23].

This paper demonstrates the dynamics of a 25mm Tenneco (Kinetic Pty Ltd) damper valve, and aims to predict valve performance. The Tenneco damper valve is characterised by several design features, some of which are tuneable. In previous studies, analytical or numerical damper models were developed for one valve configuration, and the tuneable valve parameters were not considered [4]. Coupled Fluid-Structure-Interaction simulations are time intensive and provide accurate results for only one valve configuration. This paper describes the implementation of parametric CFD modelling to capture valve performance changes. Following this study, external Tenneco valve adjustments can be investigated. However, the immediate aim of this study is to model Kinetic Suspension Systems using the predicted valve response.

In this study ANSYS CFX is used for parametric CFD modelling to predict the performance of the Tenneco damper valve. The CFD results are coupled with an analytical valve model within Matlab to determine the valve pressure differential for a given flow rate. The three main requirements of this study are,

- i) To apply parametric CFD analysis to map the valve fluid dynamic performance,
- ii) To calculate valve deflection analytically for a given pressure distribution, and
- iii) To couple the CFD results and analytical calculation and evaluate the valve performance curve

Background Damper

Dampers use hydraulic effects to resist transient wheel motion during vehicle manoeuvring, thereby improving tyre contact with the road surface. This controls the tyre's lateral load capacity, which governs the vehicle's transient handling balance [3].

The ability to quickly tune dampers without physical testing is important in motorsports. While production car dampers are not adjustable due to manufacturing constrictions, motorsport dampers have internal and external valve adjustments to achieve the maximum possible tyre grip [16]. Through the physical understanding of damper valve and adjustment behaviour, models can be developed to predict damper performance without testing.

The basic damper layout is illustrated in Figure 1 below. The major parts are the bump (compression) chamber, rebound (extension) chamber, damper valve and accumulator (or reservoir). The valve generates a pressure differential between the bump and rebound chambers as the piston forces fluid through the valve. The pressure differential acting on the piston face provides a damping force. The accumulator pressurises the hydraulic system, ensuring that the lowest pressure is above vapour pressure to avoid cavitation. Also, the accumulator accommodates the change in system volume as the piston rod enters the damper.

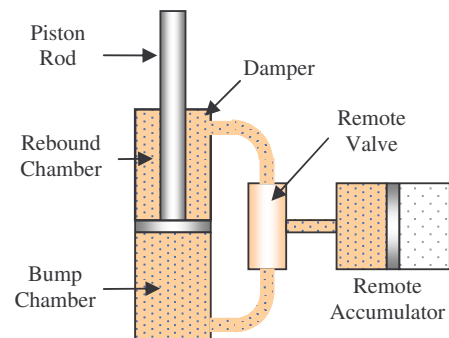


Figure 1. Kinetic Suspension single damper layout

Damper Valve

The damping force is controlled by the pressure differential across the damper valve for a given flow rate. Therefore the valve pressure differential characteristics govern the overall damper performance. Furthermore, the pressure differential and flow relationship are dictated by the coupling of the elastic response of the deformable valve structure to the fluid flowing through the valve [18].

The shearing of hydraulic fluid that flows through various restrictions in the valve forms the main damping mechanism. This fluid shearing dissipates energy in the form of heat [16]. The three main forms of fluid shear to produce the desired damping force are bleed leakage, orifice restriction and blow-off flow. The bleed and blow-off are in parallel, and together they are in series with the orifice restriction [5].

The bleed is a fixed area orifice that is highly restrictive, dominating the damping at low flow rates (low piston speeds). This orifice allows fluid to bypass the deformable valve structure. This controls the vehicle handling balance for low frequency manoeuvring [5]. Both the bleed and orifice restriction are passive features that induce a turbulent flow regime, where the pressure drop is nearly a quadratic function of flow [5]. Energy is contained in the turbulent flow as velocity fluctuations. Fluid viscosity causes these velocity fluctuations to die out, converting fluid turbulent kinetic energy into heat [13].

Thin shims and a spring preloaded disc (blow-off disc) prevent the fluid in the damper from exiting the main flow orifices. The combined shim and spring stiffnesses and preloads are designed to provide a controlled annular flow path at mid-high flow rates. Thus the shim and spring deflection dominate the valve pressure differential at mid-to-high flow rates [16]. This annular flow passage decreases the valve pressure differential at higher piston speeds, increasing tyre response. This flow regime is known as blow-off, creating a distinct kink in the damping curve as the damping decreases.

The shim stack, preloaded from the blow-off disc, obstructs the orifice flow passage until sufficient pressure differential exists to deform the structure. Hence, the shim stack and spring can be preloaded to prevent deformation until a desired pressure differential is reached [16]. In combined shim and spring valve designs, the blow-off sharpness (as preload is overcome) can be tuned using the shims [14].

The damper valve studied in this paper is the non-externally adjustable 25mm Tenneco Automotive (or Kinetic Pty Ltd) valve, seen in Figure 2.1. Unlike conventional damper valves, both shims and a spring preloaded disc control fluid flow in the Tenneco valve. Therefore, the deflection of both the shims and spring are dependent on the flow-rate through the valve. The Tenneco valve restricts fluid flow in one-direction, with a check valve for opposing flow.

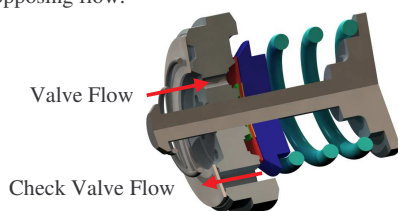


Figure 2.1. 25mm Tenneco Automotive valve cutaway view

Another fundamental feature of this valve is the shims which mate on an inner and outer land adjacent to a radial groove. This radial groove, seen in Figure 2.2, assists in equalising the

stagnation pressure beneath the shims for a uniform and predictable pressure distribution and shim deflection.

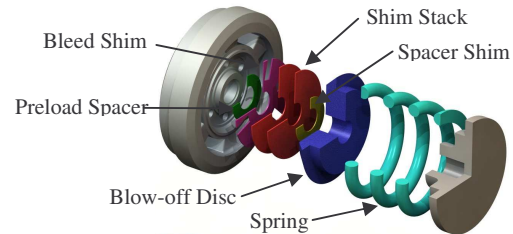


Figure 2.2. Tenneco valve detailed cutaway view

Internal valve adjustments involve varying the coil spring stiffness and preload that acts on the blow-off disc. Further valve adjustment is allowed by varying the shim stiffness, maximum deflection and preload. Firstly, the shim stiffness is controlled by the thickness and quantity of shims (where more and thicker shims are stiffer). Secondly, maximum deflection is restricted by a spacer shim between the shims and the spring preloaded disc. Finally, shim preload is governed by the thickness of a lower spacer shim situated between the lower face of the shims and the inner valve land. Notably, the inner land has a dimensional offset relative to the outer land. Furthermore, the maximum allowable shim preload is limited by the spring preload acting on the blow-off disc (this forces the shims against the lower spacer shim). All these parameters are shown above in Figure 2.2. Therefore, damper tuning requires adjustment of all these parameters, which include deformable structure stiffness and preload, orifice area and bleed area [16].

Numerous mathematical and numerical (CFD and Fluid-Structure-Interaction (FSI)) models have been developed to model the performance of damper valves. However, few models capture the complex valve fluid dynamics and accurately predict the pressure loading on the deformable valve structure.

LaJoie [10] found the complex flow within the valve presented difficulties in determining the actual force on the deformable structure. Factors were used to correct the inaccuracies, but the correction factors needed continual adjustment. Duym, Stiens and Reybrouck [6] used a mathematical approach to model valve performance, but errors were introduced when accounting for the flow distribution between parallel valve channels. Similarly, Duym, Stiens, Baron and Reybrouck [5] investigated the hysteretic behaviour of dampers using an analytical model. They concluded that the model predictive power could be improved with valve fluid modelling. Herr, Mallin, Lane and Roth [8] calculated the dynamic discharge coefficient of a damper valve by applying CFD, and later used this coefficient to model a single damper in Easy5 (schematic based virtual prototype development software, commonly used to model hydraulic systems). Talbot and Starkey [16] focused on the tuneable valve parameters within an analytical damper model. They found that the complicated valve flow path makes mathematical modelling difficult. The model relied on simplifying assumptions to couple the flow field to the deformable structure. Rifai, Buell and Johan [15] used FSI to model the interactions in a damper valve. They found that the complex geometry makes it impractical to determine the stress distribution on the deflected parts. Furthermore, hysteresis was not investigated. Likewise, Zhenhua, Zhuo and Shimin [23] used FSI to analyse the coupling characteristics of a damper valve structure. Minimal hysteresis was observed in the transient valve response. Notably, the simulations used a laminar flow model and simplified valve geometry to increase simulation speed. It was recognised that detailed CFD is required to capture all the valve characteristics.

The combined shim and spring deformable structures found in the Tenneco valve is investigated only infrequently in the damper literature. Also, few models capture valve adjustment within both the shim and spring configurations.

Application of CFD

Computational Fluid Dynamics (CFD) is used to investigate the pressure distribution acting on the deformable valve components and the pressure differential across the valve. ANSYS CFX v11 is selected for CFD modelling as it incorporates parametric modelling through the DesignXplorer environment. Valve parametric modelling allows the pressure distribution and valve pressure differential to be evaluated at numerous flow rates and valve deflections.

CFD includes turbulence models to account for fluctuating flow velocities during turbulence. Conversely, Reybrouck [14] modeled the turbulent flow through high Reynolds number sections within a damper valve analytically, assuming a constant velocity over the section. Furthermore, nearly all analytical models assume a constant discharge coefficient.

Geometry and Boundary Conditions

The properties of a fluid combined with the geometric flow resistances describe the fluid dynamics of a system [10]. In this study Kinetic LDS oil is the operating fluid, with a density of 860kg/m^3 and viscosity of 25mPas at 25°C . This incompressible, viscous Newtonian fluid is assumed to have temperature independent density and viscosity consistent with [7,9], so the model is assumed to be isothermal with a temperature of 25°C .

The valve geometry is modelled in SolidWorks, and all dimensions interlinked to ensure stability of the valve geometry during parametric updates. The valve has 8 orifices, so cyclic symmetry is applied where the model geometry captures a single orifice, see Figure 3. Eight orifices are chosen so that the deformable structure predominantly controls the valve flow restriction, rather than the orifice flow. Furthermore, the check valve is excluded as its pressure differential is assumed to be relatively minimal.

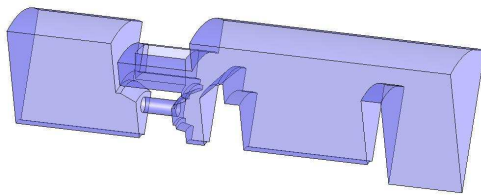


Figure 3. 1/8th valve geometry, prior to importing into CFX

The main boundary conditions applied to the model are a constant mass flow rate inlet and constant pressure outlet. These boundary conditions are consistent with previous numerical valve studies [6, 9, 18, 19 and 23]. Similar to [7], the walls are assumed to have no-slip [7] and symmetry boundary conditions are applied to the sides of the geometry.

The parametric modelling varies the mass flow rate inlet for each valve geometry, where the valve geometry is progressively incremented. The flow rate values are selected to provide high resolution at low flow rates (where damping is most crucial) and fewer at high flow rates where the damping changes the least.

The outlet pressure represents the accumulator pressure acting on the hydraulic valve. However, the constant pressure outlet does not exactly represent the valve physical behaviour. In practice, this pressure varies depending on rod displacement into the damper. Additionally, in a H2-Kinetic Suspension System the

accumulator pressure fluctuates with vehicle roll. Therefore, a sensitivity analysis revealed that the distributed pressure varied 0.55% for a 15bar difference in outlet pressure. Similarly, Duym, Stiens and Reybrouck [6] found the fluctuating accumulator pressure provides less than 5% error.

Till and Wendel [19] applied a zero pressure condition at the outlet boundary condition to easily calculate the valve pressure drop. However, the pressure differential can be easily calculated using the CFX-Expression-Language (CEL) in the post processing environment. As a result, the outlet boundary condition can represent a practical value; in this case the pressure is set to 10bar, a typical damper accumulator pressure.

ANSYS CFX is capable of modelling bubbles within the fluid, as experienced during cavitation. These entrained bubbles are the basis of hysteresis in damper performance [21]. This valve application is for Kinetic Suspension Systems where twin accumulators pressurise each side of the piston. This reduces the possibility of cavitation, so the cavitation bubbles are omitted from the model.

CFX Mesh

Three geometric simplifications are applied prior to meshing, to reduce the local mesh density and decrease solving time. Firstly, the coil spring is removed from the geometry. The spring is located downstream of the orifice restrictions in a large flow field, so it has minimal influence.

Small flow paths require high mesh refinement, greatly increasing the mesh density and solving time. To simplify the geometry for meshing, the bleed area is modelled as an initial offset of the blow-off disc. A slotted shim allows the bleed leakage flow through the Tenneco valve. The offset blow-off disc creates an annular flow passage area equivalent to the area of the slots. This offset increases the initial fluid path, thus reducing the need for higher mesh refinement. Tallec and Mouro [18] automatically set the flow rate to zero for all fluid cells that are too thin, such as when the valve deflection approaches zero. This assumption underestimates the fluid path section and thus over estimates the pressure differential at these deflection values.

The limited shim deflection is small relative to the shim diameter, so the shims are assumed to be perpendicular to the fluid flow. Therefore, the third simplification is the removal of the shims in the geometry, and only the blow-off disc is modelled.

These geometric simplifications permit higher mesh refinement in critical locations without compromising solving time. Critical areas requiring finer meshes are where physical quantities vary a lot [7]. Such areas include the region around the orifice entry and exit, and clearance between the blow-off disc and the valve land. For the latter, proximity mesh refinement is applied to increase the mesh density between the two neighbouring surfaces. The refined mesh ensures a mesh independent solution [9], and a mesh convergence analysis is used to determine the global mesh size.

Controlling the number of elements during the mesh convergence analysis is difficult due to the complex 3D geometry. A slight variation in mesh size generates large variations in element numbers. Figure 4.1 below illustrates the number of elements, solve time and relative result accuracy for four different global mesh sizes. Figure 4.1 also includes the relative pressure error of a grid refinement analysis, revealing up to 6.5% error. This result indicated the refinement required at critical model boundaries. The mesh size is also dictated by the consistency of the results, which influences the stability of the analytical model coupled to

these results. Figure 4.2 shows the resulting oscillatory behaviour of a coarse mesh.

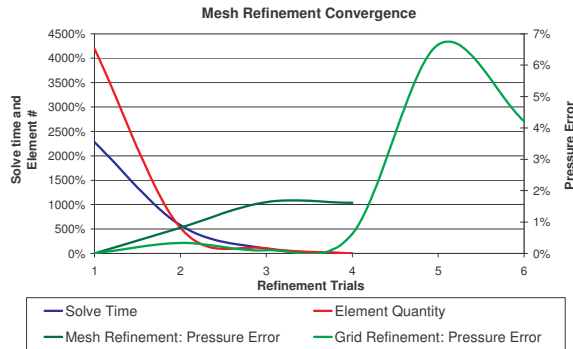


Figure 4.1. Element quantity, solve time and result accuracy

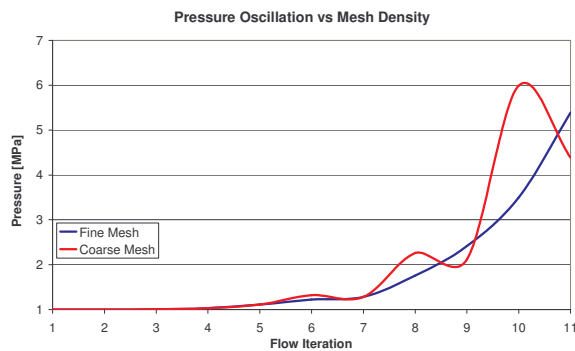


Figure 4.2. Result behaviour of a fine and coarse mesh density

Prior to parametric modelling, the initial mesh is configured for the smallest valve deflection (i.e. highest mesh refinement). This ensures the configured mesh is satisfactory for the automatic re-meshing that takes place during parametric modelling. Moreover, the geometry at the largest valve deflection is meshed to verify the mesh quality.

The final 3D mesh, shown in Figure 5, has 229,452 elements and 60,195 nodes, with 183,771 Tetrahedrals, 269 Pyramids and 45,412 Prisms. The boundary layer is 5 elements thick.

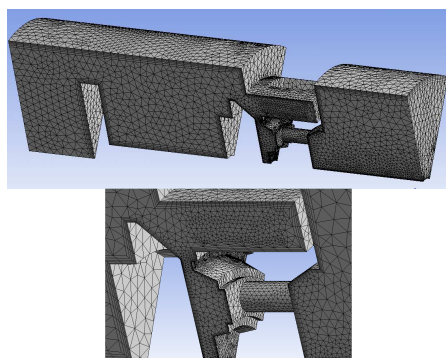


Figure 5. Overall valve mesh and proximity refinement

CFD Solving

The CFD simulation type is steady state, so as to efficiently evaluate the valve pressure information for each geometry increment.

At the highest flow rate, the Reynolds number for the valve is calculated to be 11,500 for the orifice and 3,800 for the annular flow path. Therefore, the simulation is solved using the

Reynolds-averaged Navier-Stokes (RANS) equations as this models a wide range of turbulence scales and provides a fast solution. The relatively small and complex valve geometry limits the mesh refinement for critical regions, such as the annular flow path. With insufficient mesh refinement Large-Eddy-Simulation (LES) yields an inaccurate solution. Also, the desired high mesh density would increase computation time, hence yielding LES unsuitable [13]. Direct Numerical Simulation (DNS) solves the Navier-Stokes equations without modeling turbulence, but the geometry is far too complicated for DNS and the computing resources required would be prohibitive in this case [13].

RANS is a low end CFD modelling technique, typically requiring physical verification [13]. The equations require a turbulence model for the Reynolds stress terms. Rifai, Buell and Johan [15] used a variation of the Spalart-Allmaras (S-A) turbulence model in their FSI simulations. However, they simplified the valve geometry and studied damper cavitation for production car NVH purposes.

The k-ε turbulent model is often used for Reynolds numbers above 1000 [9]. However, this turbulence model and the Baseline k-ω fail to account for the transport of turbulent shear stress under high pressure gradients [2]. These pressure gradients are evident in damper valves at the entrance to the orifices and the annular flow path. Therefore, the two-equation k-ω based Shear-Stress-Transport (SST) turbulent model was employed. This model accurately predicts flow separation at high pressure gradients, typically seen in damper valves [2].

CFD Post-Processing

The pressure distribution on the blow-off disc and the valve pressure differential are required to couple with the analytical valve model. CFX post-processing calculates the nodal-average pressure distribution acting on the face of the blow-off disc and the inlet and outlet nodal-averaged pressure difference.

The average pressure distribution is assumed to be acceptable for calculating the deflection of the valve structure, as the shim deflection is relatively small. This small deflection indicates that the stagnation pressure acts on a face almost perpendicular to the fluid flow. Furthermore, the small deflection reduces the non-uniform shim deflection due to pressure distribution inconsistencies. Finally, this assumption is applicable for the Tenneco valve, as the radial groove beneath the deformable structure tends to equalise the stagnation pressure below the blow-off disc.

Analytical Models

The purpose of the analytical models is to calculate the valve deflection for a given pressure distribution and to couple this valve deflection to the CFD results. The coupling between the analytical valve deflection and CFD results determines valve equilibrium and then outputs the overall pressure differential. From this coupling model the valve performance curve can be established, relating pressure differential to flow rate.

Valve Deflection Model

The stiffness of the deformable structure controls the damping characteristics, so it is vital to include all main functions of the valve deflection [16]. The valve deflection is separated into two fields, the deformable structure stiffness and the load acting on this structure. LaJoie [10] found the load on the valve structure to be a function of shim stack area, static pressure, fluid dynamic pressure and upstream chamber pressure. For the valve modeled in this paper, the upstream chamber pressure is the accumulator pressure, assumed to be constant throughout the CFD simulations.

Talbot and Starkey [16] identified four forces acting on a valve structure: the distributed pressure on the valve face, valve preload caused by the shim stack, valve force for a given deflection (given the valve stiffness) and fluid momentum. Furthermore, they identified and neglected valve inertia and friction in their models. This assumption seems to be valid for this study as the Tenneco valve is mounted externally on Kinetic Suspension Systems. This eliminates the valve component movement with the damper piston during wheel motion. Also, Tallec and Mouro [18] neglected valve inertia, and Lang [11] found that valve inertia has almost undetectable influence.

The fluid momentum term is not included in this deflection model as the CFD results are processed for incremental steady state flow conditions. For this reason, the hysteresis behaviour is not captured in the model, likewise for Talbot and Starkey [16]. Finally, the check valve is ignored as it is assumed to provide very little flow restriction, comparable to Duym, Stiens, Baron and Reybrouck [5].

Bleed Leakage

The valve bleed leakage is modelled as an initial valve deflection. This deflection is calculated using the equivalent annular flow area from the hydraulic diameter. This initial deflection is added to the actual valve deflection to represent the bleed throughout the entire valve performance curve.

Zhenhua, Zhuo and Shimin [23] and Gao [7] found that leakage between the valve shaft and the deformable structure (blow-off disc) was a cause of error. Using the equivalent area technique the leakage can be accounted for by the addition of another initial deflection. For instance, a 0.05mm clearance is equivalent to a 0.0072mm initial deflection, which is then added to the previous offset.

Shim Stack Deflection

The shim stack dynamics are determined by calculating the shim tip deformation. The shim tip deformation generates an annular flow path for the fluid. The shim stack deflection is evaluated using the shim stack stiffness and the pressure distribution [16].

The shim stack deflection is less critical for Tenneco damper valves compared to conventional valves. With the Tenneco valves, a spacer shim limits the maximum shim deflection. As the shims are not the primary source of valve deflection, the shim deflection is relatively low.

Talbot and Starkey [16] showed that the valve shim stack can be successfully modelled using stacked thin discs. Also, Herr, Mallin, Lane and Roth [8] demonstrated through CFD modelling that a constant pressure distribution acting on the shim face is a valid assumption to model shim deflection. This is consistent with the Tenneco valve, as the radial groove equalises the pressure distribution beneath the shims.

The shim deflection was calculated using a superposition technique similar to Talbot and Starkey [16]. The shims were modelled using the bending equations for uniform thickness circular plates from Young and Budynas [22]. Superposition was applied to the shim stack, coupling the deflection of neighbouring shims to resolve the effective stiffness of the stack. The deflection of each shim is calculated from the reaction force from neighbouring shims. However, the lower shim deflection calculation also includes the pressure distribution that acts on the shim stack. The deflection equations are then equated at the locations where shims contact one another. Inter-shim friction is not investigated within this model, although it is suspected to have a contribution to the overall valve hysteresis.

Talbot and Starkey [16] made several assumptions to model the shim stack behaviour. As the flow field around the shim stack was not well understood, the pressure distribution was assumed to operate over an estimated area. Secondly, the circumferential shim deformation was assumed to be discontinuous, so a reduced deformation was assumed. Other valve models have assumed the pressure distribution acting on the shim face to be confined to a region similar in size to the orifices. This study avoided these assumptions by using the average pressure distribution (from CFD) for the valve model.

The shim model limits maximum shim deflection by incorporating the spacer shim. In this model it is assumed that the shims bend at a diameter that exceeds the spacer shim outside diameter. This assumption is justified as the spring preload fixes the inner edge of the shim between the spacer shim and the valve. Therefore, fixed inner edge bending equations are used throughout the model.

Shim preload is modelled, with the preload limited by the thickness of the preload spacer. However, the spring preload acts on the shim stack through the blow-off disc and spacer shim, so the maximum shim preload is strictly governed by the spring preload. Thus, if the spring preload is insufficient, the model reduces the maximum allowable shim preload accordingly.

Spring Preloaded Disc Deflection

The blow-off disc deflection is modeled using a simple linear stiffness, preloaded spring model. The model allows for an adjustable spring preload. The maximum spring compression until coil binding is calculated according to the specified preload. The spring preload is modeled as it greatly influences the valve performance, dictating the blow-off point or the transition between low and high speed damping. Finally, the blow-off disc deflection is added to the shim stack deflection and the bleed offset to represent the overall deflection of the valve for a given pressure distribution.

Analytical Deflection and CFD Coupling Model

Parametric CFD modelling sequentially updates the geometry and simulation to map the valve's fluid dynamic performance for varying geometry and flow rate conditions. The fluid dynamic performance is indicated by the valve pressure differential and pressure distribution for a given flow rate and valve deflection. Moreover, the analytical valve deflection is calculated for a given pressure distribution acting on the deformable valve structure. Therefore, the purpose of this model is to numerically couple the analytical valve deflection with the CFD pressure results to map the non-linear valve performance.

The model is a quasi-static analysis of the fully coupled valve system. The CFD data and the valve adjustment parameters are the model inputs. The model solves the valve pressure differential at discrete flow increments, matching those modelled in CFD. Similar to Duym, Stiens and Reybrouck [7], the hysteresis and fluid momentum terms are not captured in the quasi-static model.

Numerical techniques are used to converge the solution at valve equilibrium, where valve deflection and pressure distribution are balanced. The Jacobi Method which determines the solution for the n^{th} iteration using the results from the $(n-1)^{\text{th}}$ iteration is used in this coupled problem. Eventually the solution converges as the error reduces, although there are cases of convergence instability.

The deflection model includes both shim and spring deformation and preloads, making the interaction discontinuous. Oscillating

the CFD results for each flow rate is detrimental to solution convergence. Both discontinuities and oscillating results created inappropriate solutions through convergence instability. Therefore, relaxation techniques are used within the model to control the solution stability. Likewise, Talbot and Starkey [16] successfully implemented relaxation techniques to improve convergence when using Newton's method.

An under-relaxation value (i.e. $\omega < 1$, in equation 1) is applied to eliminate convergence oscillations. Maximum convergence stability is achieved when the relaxation factor is variable, changing as a function of valve stiffness and preload. This is attributed to the high growth in CFD pressure results at low valve deflections (i.e. when the valve stiffness is high). Furthermore, a polynomial interpolation is used in the model as a second order polynomial best characterises the CFD results.

$$\phi^n = \phi^{n-1} + \omega (\phi_{interp}^n - \phi^{n-1}) \quad (1)$$

For the first iteration, the model commences with selection of an arbitrary distributed pressure value within the list of pressure results at the flow-rate increment. Using this pressure distribution, the valve deflection is calculated analytically. The new deflection value is used to interpolate the pressure distribution. However, the pressure distribution for the next iteration is calculated using equation (1). This loop concludes when the RMS error criterion between two consecutive iterations of the deflection is met.

The overall valve pressure differential is then interpolated for this converged equilibrium point. This process is then repeated for the remaining flow-rate increments. Figure 6 below displays the flow chart of the convergence algorithm.

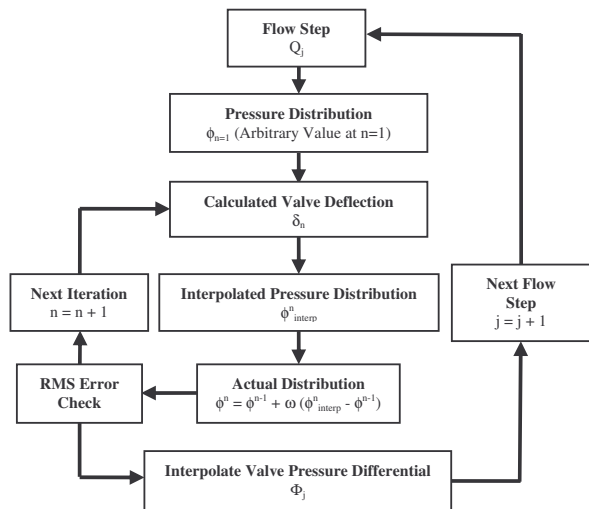


Figure 6. Coupling algorithm flow chart

CFD Results

The parametric modelling completed 120 steady state CFD simulations, each requiring 20 minutes solve time. Approximately 40 hours was required to map the valve fluid performance. Conversely, only one valve configuration is simulated in each FSI simulation, so when the valve parameters are modified, the simulations need to be repeated.

Flow Visualisation

The valve flow characteristics are visualised through the use of a mid-plane velocity contour plot and streamlines, similar to Till and Wendel [19]. The streamlines seen in Figure 7 reveal the

vena-contracta constriction just downstream from the main orifice entry. This reduces the effective flow passage at the orifice entry. Also, the streamlines indicate that the flow field has minimal disturbance around the spring region so excluding the spring from the model is justified. Figure 8 shows the high fluid velocity through the orifice that decreases before reaching a stagnation point on the blow-off disc.

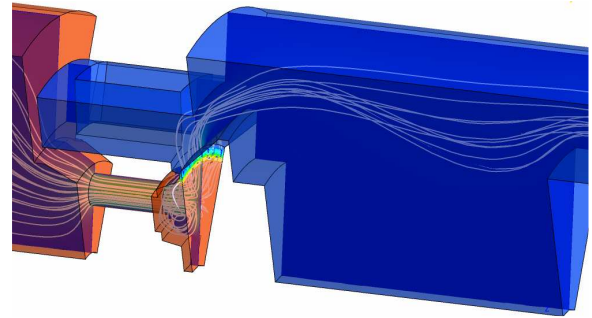


Figure 7. Valve flow field visualisation

Figure 7 also shows that the fluid volume appendage above the orifice (for check valve fluid flow) has minimal contribution to the flow. However, at high flow rates this region is associated with fluid re-circulation, which reduces the development of a low pressure region adjacent to the blow-off disc.

Pressure Distribution and Differential

The pressure results are illustrated using geometry transparency with a colour contour representing the varying pressure regions (Figure 8).

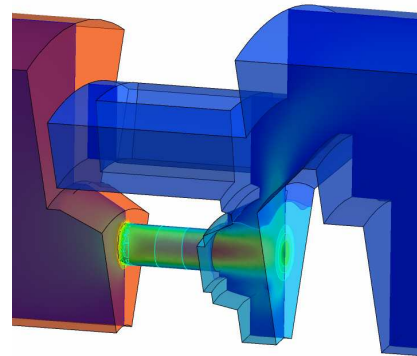


Figure 8. Valve pressure distribution and differential

Figure 8 shows that the pressure distribution on the blow-off disc stretches laterally. This lateral stretch is caused by the radial flow groove beneath the blow-off disc equalising the stagnation pressure distribution. The pressure distribution peak size is comparable to the size of the piston orifice, as recognised by Herr, Mallin, Lane and Roth [8]. The streamlines in Figure 7 highlight that the fluid flows laterally into the groove at the stagnation point just beneath the disc.

From the geometry colour in Figure 7, the blow-off disc generates the main pressure differential at smaller deflections and the orifice becomes the main flow restriction, as seen in Figure 8. As the valve approaches maximum deflection the pressure increase (as a function of flow) is almost parabolic. Talbot and Starkey [16] found the valve shim stack is the primary cause of pressure drop across the valve. As they only modelled the shim stack, the valve deflection is small, so it becomes the critical flow path.

The pressure plot also reveals that the majority of the orifice pressure drop occurs at the opening, where the fluid velocity rapidly increases. Figure 8 shows that a marginal pressure drop occurs over the orifice length due to turbulence.

Analytical Valve Deflection Results

The valve deflection is the clearance between the valve outer land and the outer edge of the lowermost shim. This clearance defines the annular fluid flow path and depends on the deformation of both the shims and the blow-off disc. Figure 9 below displays the combined valve deflection.

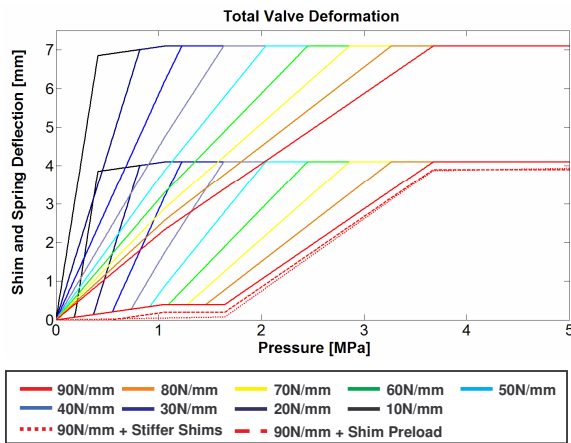


Figure 9. Valve deflection versus pressure distribution

The different coloured curves represent the valve deflection characteristics over a range of spring rates, from 10 to 90N/mm. There are two groups of curves, with and without spring preload, where spring preload requires an initial spring deflection. This initial deflection reduces the maximum spring deflection before coil binding. From Figure 9, the same rate of valve deflection occurs in both cases but is initiated at a lower pressure in the case where there is no spring preload, and a larger deflection results. Shim deflection can be identified as the lower, stiffer deflection observed prior to the spring deflection for the preloaded case, although it is noted that shim and spring deflections can occur simultaneously. For valve configurations with no spring preload, the shim deflection is disguised by the spring's high rate of deflection.

The deflection appears to be linear due to both the shim and spring deflection being a linear function of the pressure distribution. However, the shim stack deflection is non-linear across its radius. The deflection curve for the spring preload case is discontinuous because the individual shim and spring preloads must be overcome prior to deflection. In practice the shims smooth out this discontinuity. The shim preload should reduce as the spring deflects as the pressure is increased. The relieved shim preload allows premature shim deflection just as the spring preload is overcome. However, the model retains the initial shim preload as the spring deflects. This is valid if the spring preload exceeds that of the shim. In addition, the maximum shim preload is limited by the spring preload, so shim and spring deflection will commence simultaneously after the spring preload is overcome, independent of shim stiffness.

The deflection characteristics for varying shim stiffness and preload for the 90N/mm spring rate is shown in Figure 9 for the case with spring preload (lower red curve). For higher shim stack stiffness (dotted red curve) the shim continually deforms throughout the pressure cycle, even after the blow-off disc coil binds. Added shim preload (dashed red curve) delays the shim

deformation until a higher pressure, and the overall valve deflection is reduced from the initial shim deflection for preload.

Coupled CFD and Analytical Valve Results

The parametric CFD simulation is executed once and the coupled post-processing predicts the valve performance incorporating different tuneable parameters. However, if the orifice diameter and/or orifice number are varied, an updated parametric simulation must be executed. The coupling post-processing takes approximately 20 seconds per valve configuration.

After coupling the deflection characteristics with CFD results, it is seen that the deflection difference between spring rates increases for higher flow rates, as illustrated in Figure 10. This is due to the parabolic increase in the pressure distribution as the flow rate is incremented. The figure also displays a steep, initial and final valve deflection gradient, but a shallower deflection gradient for the mid flow rate range. This is due to the higher spring stiffness compared to the shim stack after preload is overcome.

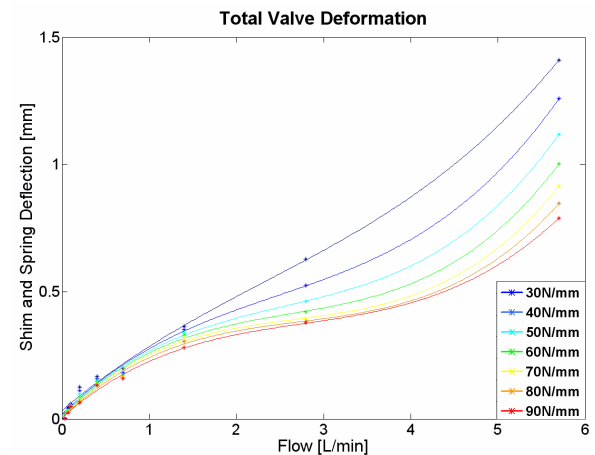


Figure 10. Deflection versus flow for spring rates (30-90N/mm)

Figure 11 shows the initial pressure differential increase until the preload is overcome and the blow-off disc begins to deflect. This portion of the curve involves both bleed flow and shim flow. Beyond 12 L/min flow rate the valve deflection is large and the orifice flow restriction becomes dominant, and the pressure increases rapidly with flow. Figure 11 also shows a decrease in the overall valve pressure differential for increased bleed flow. This effect is less evident at higher flow rates as the bleed deflection is small compared to the overall valve deflection.

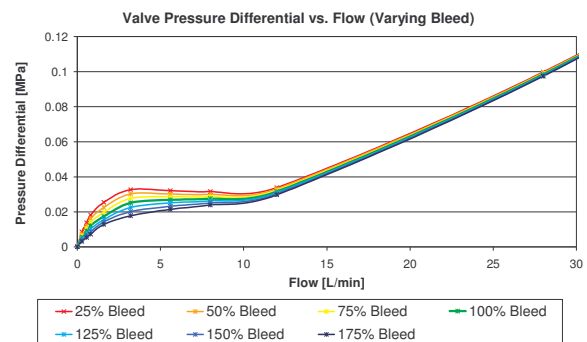


Figure 11. Valve performance plot, varying bleed orifice

Figure 12 shows the performance curve for different spring rates and also shows the minimum and maximum curve limits from

varying spring preload. It was recognised, similar to Talbot and Starkey [16], that higher preload increases the pressure differential over the entire curve. Increasing the preload also shifts the blow-off point to a higher flow rate where the pressure distribution is also higher.

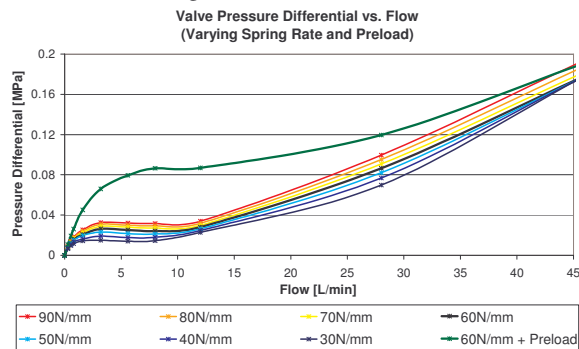


Figure 12. 30-90N/mm spring rates and preload curve

Valve preload creates deflection discontinuities. This instantaneous rate of change in deflection causes a pressure differential trough after blow-off, shown in both Figure 12 and 13. Zhenhua, Zhuo and Shimin [23] also observed this in their FSI simulations.

Overall, the valve performance at low and high flow rates behaves as expected. Namely, the pressure differential decreases with added bleed leakage and/or reduced spring rate, and blow-off occurs at higher flow rates with added preload.

Conclusions

This paper presents the valve performance curves obtained by combining both numerical and analytical techniques. The valve deflection, component pressure distribution and overall valve pressure differential are investigated. The combined numerical and analytical technique provided a fast valve performance solution whilst allowing crucial parameters to be adjusted.

The results in this paper indicate that damper valve performance can be predicted including most tuneable parameters. These conclusions suggest that Fluid-Structure-Interaction simulations are less feasible to simulate varying valve parameters. Nonetheless, FSI simulations are recommended for investigating higher order effects in transient valve response analysis. Future research that implements friction, valve inertia and other high order effects within the analytical model in this study could simulate transient valve response, such as hysteresis.

Because the numerical modelling involves the RANS equations, simulation verification is recommended. Also, the shim and spring preload dynamics are difficult to model analytically, providing localised inaccuracies. Therefore, future study into Particle-Image-Velocimetry (PIV) experiments would provide fundamental data to verify the CFD and valve deflection results.

References

- [1] Anderson, J.D., *Computational Fluid Dynamics – The Basics with Applications*, McGraw-Hill, Singapore, 1995.
- [2] ANSYS Inc., *ANSYS CFX, Release 11.0 Help, Turbulence and Wall Function Theory*, ANSYS Inc. 2007.
- [3] Dixon, J.C. 1999, *The Shock Absorber Handbook*, Society of Automotive Engineers, Warrendale, USA.
- [4] Duym, S.W., Simulation Tools, Modelling and Identification, for an Automotive Shock Absorber in the

- Context of Vehicle Dynamics, *Vehicle System Dynamics*, **33**, 2000, 261-285.
- [5] Duym, S.W., Stiens, R., Baron, G.V. & Reybrouck, K.G., Physical Modelling of the Hysteretic Behaviour of Automotive Shock Absorbers, *SAE technical paper No. 970101*, Society of Automotive Engineers, 1997.
- [6] Duym, S.W., Stiens, R. & Reybrouck, K.G., Evaluation of Shock Absorber Models, *Vehicle System Dynamics*, **27**, 1997, 109-127.
- [7] Gao, D., Investigation of Flow Structure Inside Spool Valve with FEM and PIV Methods, *International Journal of Fluid Power*, **5**, 1, 2004, 51-66.
- [8] Herr, F., Mallin, T., Lane, J. and Roth, S., A Shock Absorber Model Using CFD Analysis and Easy5, *SAE technical paper No. 1999-01-1322*, Society of Automotive Engineers, 1999.
- [9] Kim, C., Perng, C.Y. & Zhang, D., Transmission Main Control Orifice Flow Characteristics and Correlations, *SAE technical paper No. 2004-01-1639*, Society of Automotive Engineers, 2004.
- [10] LaJoie, J.C., Damper Performance Development, *SAE technical paper No. 962551*, Society of Automotive Engineers, 1996.
- [11] Lang H.H., A study of the characteristics of Automotive Hydraulic Dampers at High Stroking Frequencies, PhD Dissertation, The University of Michigan, 1977.
- [12] Leap Australia, *DesignModeler and CFX-Mesh Training Manual*, Leap Australia, 2005.
- [13] Ranasinghe, J., *Lecture Notes: Computational and Experimental Fluid Mechanics*, University of Western Australia, 2007.
- [14] Reybrouck, K., A non linear parametric model of an automotive shock absorber, *SAE technical paper No. 940869*, Society of Automotive Engineers, 1994.
- [15] Rifai, S.M., Buell, J.C. & Johan, Z., Automotive Engineering Applications of Multi-physics Simulation, *SAE technical paper No. 1999-01-1022*, Society of Automotive Engineers, 1999.
- [16] Starkey, J. & Talbott, M.S., An Experimentally Validated Physical Model of a High-Performance Mono-Tube Damper, *SAE technical paper No. 2002-01-3337*, Society of Automotive Engineers, 2002.
- [17] Surace, C., Worden, K. & Tomlinson, G.R., An Improved Nonlinear Model for an Automotive Shock Absorber, *Nonlinear Dynamics*, **3**, 1992, 413-429
- [18] Tallec, P.L. & Mouro, J., Fluid Structure Interaction with Large Structural Displacements, *Computer Methods in Applied Mechanics and Engineering*, **190**, 2001, 3039-3067.
- [19] Till, L.T. & Wendel, G., Application of Computational Fluid Dynamics Analysis in Improving Valve Design, *SAE technical paper No. 2002-01-1397*, Society of Automotive Engineers, 2002.
- [20] Warner, B. & Rakheja, S., An analytical and experimental investigation of friction and gas spring characteristics of racing car suspension dampers, *SAE technical paper No. 962548*, Society of Automotive Engineers, 1996.
- [21] Yeh, C., Lu, S.H., Yang, T.W. & Hwang S.S., Dynamic Analysis of a Double-Tube Shock Absorber for Robust Design, *JSME International Journal – Mechanical Systems, Machine Elements and Manufacturing*, **40**, 2, 1997, 335-345.
- [22] Young, W.C. & Budynas R.G., *Roark's Formulas for Stress and Strain 7th edition*, McGraw Hill International, Sydney, 2002.
- [23] Zhenhua, L., Zhuo, W. & Shimin, L., Finite Element Simulation of Non-Linear Dynamic Characteristics of Hydraulic Damper's Valve, *Journal of Mechanical Strength*, **25**, 6, 2003, 614-620.